Coarse Graining the Vorticity Equation in the ECMWF Integrated Forecasting System: The Search for Kinetic Energy Backscatter

G. J. SHUTTS

European Centre for Medium-Range Weather Forecasts, Reading, and Met Office, Exeter, United Kingdom

(Manuscript received 30 July 2012, in final form 23 October 2012)

ABSTRACT

Stochastic kinetic energy backscatter parameterization schemes are now widely used in ensemble prediction systems to account for random error associated with excessive dissipation and unrepresented energy backscatter in numerical weather prediction models. This dissipation arises from numerical advection schemes and explicit diffusion terms and is also implicit in some parameterization schemes. In the absence of a backscatter theory applicable to the convective scale and mesoscale, current parameterization methods are based on simple heuristic models designed to scale the energy input in proportion to a suitable measure of net energy dissipation rate. Free parameters in the formulation of backscatter tend to be tuned for the optimal performance of ensemble prediction systems, yet other forms of uncertainty represented in these forecasting systems make that task harder. Results are presented here from a study that aims to characterize the form and magnitude of kinetic energy backscatter within a global spectral framework. This is achieved by comparing a high-resolution ''truth'' model with a spectrally truncated version of the model for which the effect of the missing scales of motion is to be gauged. Energy exchange between these omitted scales and the resolved scales of the truncated representation is computed for the dominant terms in the vorticity equation. It is found that although there is a nonlocal spectral energy flux to low wavenumbers due to the purely rotational part of the flow, it is much smaller than the dissipative effect associated with terms involving the divergent part of the flow. Biharmonic horizontal diffusion is found to contribute significantly as an energy sink across the entire wavenumber spectrum.

1. Introduction

The use of stochastic kinetic energy backscatter algorithms in meteorology was first motivated in boundary layer turbulence modeling (Leith 1990; Mason and Thomson 1992) and later by Frederiksen and Davies (1997), who brought it within the scope of numerical weather prediction. Their study focused on the form of the equilibrium energy spectra in a barotropic vorticity equation model that included stochastic backscatter and eddy viscosity parameterizations. These spectra were compared with their counterparts in direct numerical simulations (DNS) (i.e., without parameterization) at higher resolution. The inclusion of backscatter terms in the vorticity equation provided a better match of the energy spectrum to that of the DNS ''truth'' model compared to similar simulations using simpler eddy viscosity closures. Kitsios et al. (2012) extended earlier studies, based on the barotropic vorticity equation, to a two-level quasigeostrophic model and provided new scaling laws for the dependence of subgrid eddy forcing on resolution.

In the context of ensemble prediction systems (EPS) and their apparent inability to provide realistic spread, Shutts (2005) developed a stochastic kinetic energy backscatter scheme that adapted the rather simplistic ansatz of the boundary layer backscatter schemes so as to embrace the effects of convection and gravity wave/mountain drag in addition to a two-dimensional turbulence component. Unlike the 3D backscatter formulation, the concern here was with the excessive energy dissipation rate in the model's free atmosphere and within frontal zones. It was also motivated by the possibility that upscale energy cascades associated with deep convection and mesoscale convective systems are underrepresented by the combined effects of convective parameterization and explicit, near-gridscale dynamics. Similarly, it was argued that mountain drag formulations

Corresponding author address: Glenn Shutts, Met Office, Fitz-Roy Road, Exeter EX10 8BE, United Kingdom.
E-mail: glenn.shutts@metoffice.gov.uk

DOI: 10.1175/JAS-D-12-0216.1

address deficiencies in the momentum budget but act as an unrealistic energy sink.

Stochastic backscatter schemes are used in the operational ensemble forecast systems at the Met Office (Tennant et al. 2011), European Centre for Medium-Range Weather Forecasts (ECMWF) (Berner et al. 2009 for instance; Palmer et al. 2009), and Environment Canada (Charron et al. 2010). While their underlying formulations have a common spectral framework as outlined in Berner et al. (2009), rather different assumptions are made about the spectral power distribution in their respective pattern generators. The spectral power dependence on wavenumber n for the pattern generators in these implementations is

- Met Office Unified Model Global and Regional Ensemble Prediction System (MOGREPS) scheme: $n^{-1.27}$ for $5 < n < 60$, otherwise 0;
- ECMWF Integrated Forecasting System EPS: $(1 + n)^{-1.27}$ for $1 < n < 159$, otherwise 0; and
- Environment Canada global EPS: 1 for $40 < n < 128$, otherwise 0;

where n corresponds to the degree of the associated Legendre function in the spherical harmonic expansion of the pattern field. Note the very different choices of spectral range of the pattern fields and also the flat power spectrum choice in the Environment Canada EPS formulation. From a ''good science'' perspective, these formulation differences are unsatisfactory and emphasize the absence of any proven model for backscatter in the numerical weather prediction context. The $n^{-1.27}$ terms in the Met Office and ECMWF formulations are based on calculations that attempt to characterize the spectral power differences of streamfunction tendency (obtained from momentum tendencies) and their equivalents derived using coarse-grained fields (Palmer et al. 2009). A weakness of these calculations is that they do not attempt to isolate the random error contribution to tendency differences—the crucial component of a stochastic formulation. More generally, one should be concerned that the fundamental assumptions upon which operational stochastic backscatter schemes are based may be too severe—for example, the independence of the spectral components in the pattern field and its weak dependence on model flow state (through a smoothed dissipation rate).

In this paper, an attempt is made to use the ECMWF Integrated Forecasting System (IFS) to compute the effect of spectral truncation on terms in the vorticity equation and the consequent impact on the spectral energy tendencies. Powerful spectral-to-gridpoint transforms are called at each time step of a 24-h forecast to compute vorticity tendencies with full and spectrally truncated fields. Differences in the corresponding vorticity tendencies, multiplied by the vorticity itself, determine the spectral distribution of enstrophy and energy input from the truncated scales. In this way it is possible to identify backscatter and energy drain as a function of wavenumber and interpret these as necessary dynamic processes for parameterization in a model at the coarse-graining resolution. Thuburn et al. (2011) present the results of similar calculations in an idealized study using the barotropic vorticity equation and compare the computed energy drain and backscatter for different subgrid closures. They conclude that the energy drain effect is insufficiently scale selective and none of the schemes adequately represents the backscatter.

Section 2 examines the ECMWF IFS vorticity equation and defines the coarse-graining operation symbolically. Technical aspects of the calculation are described in section 3 and the results are presented and discussed in section 4. Possible implications for stochastic backscatter parameterization are suggested in section 5 with some concluding remarks and a summary given in section 6.

2. Coarse graining the vorticity equation

The aim of this coarse-graining study is to compute spectral tendency contributions in the vorticity equation using the grid-transform method and to do this with full IFS forecast fields, and then with a spectrally truncated set. The difference between the full and truncated spectral tendencies is necessarily equal to the contribution from the finer scales that are excluded by spectral truncation. These calculations are made on the fly, at every time step, during the 24-h forecasts. Note that the spectral vorticity tendencies so obtained are not identical to the ones obtained from the model's semi-Lagrangian advection scheme. In essence, the forecast model is being used to host the calculations by providing the necessary fields together with the spectral-gridpoint transform routines that greatly facilitate the computations.

a. The ECMWF IFS vorticity equation

The vorticity equation corresponding to the ECMWF IFS equations of motion (see the ECMWF documentation at http://www.ecmwf.int/research/ifsdocs/) is

$$\frac{\partial \zeta}{\partial t} + \frac{U}{a(1-\mu^2)}\frac{\partial \zeta}{\partial \lambda} + \frac{V}{a}\frac{\partial \zeta}{\partial \mu} + \dot{\eta}\frac{\partial \zeta}{\partial \eta} + \frac{1}{a}\left(\frac{1}{1-\mu^2}\frac{\partial \dot{\eta}}{\partial \lambda}\frac{\partial V}{\partial \eta} - \frac{\partial \dot{\eta}}{\partial \mu}\frac{\partial U}{\partial \eta}\right) + D(2\Omega\mu + \zeta) + \frac{2\Omega}{a}V + \frac{R_d}{a^2}J\left[\frac{T_v, \ln(p)}{\lambda, \mu}\right] = K\nabla^4\zeta + \mathbf{k}\cdot\nabla\times\mathbf{F}, \quad (1)$$

where the "vorticity" ζ is given by

$$\zeta = \frac{1}{a}\left(\frac{1}{1-\mu^2}\frac{\partial V}{\partial \lambda} - \frac{\partial U}{\partial \mu}\right) \tag{2}$$

and the horizontal divergence D is given by

$$D = \frac{1}{a}\left(\frac{1}{1-\mu^2}\frac{\partial U}{\partial \lambda} + \frac{\partial V}{\partial \mu}\right), \tag{3}$$

where a is the earth's radius and (U, V) is the horizontal wind vector multiplied by the cosine of latitude. Note that ζ is not a true component of the vorticity vector as it is computed on model levels using horizontal wind components. Also, λ is longitude, μ is the sine of latitude, η is the model's vertical coordinate defined in terms of pressure p and surface pressure p_s, Ω is Earth's rotation rate, R_d is the gas constant for dry air, T_v is the virtual temperature, K is the biharmonic diffusion coefficient, F_h is the parameterized horizontal force, and $J(\cdot)$ is the Jacobian. For model levels that are functions of p alone, the Jacobian term, which represents baroclinic generation of vorticity, vanishes.

Equation (1) can be written in the form

$$\frac{\partial \zeta}{\partial t} + \frac{1}{a(1-\mu^2)}\frac{\partial [U(2\Omega\mu + \zeta)]}{\partial \lambda} + \frac{1}{a}\frac{\partial [V(2\Omega\mu + \zeta)]}{\partial \mu} + \dot{\eta}\frac{\partial \zeta}{\partial \eta} + \frac{1}{a}\left(\frac{1}{1-\mu^2}\frac{\partial \dot{\eta}}{\partial \lambda}\frac{\partial V}{\partial \eta} - \frac{\partial \dot{\eta}}{\partial \mu}\frac{\partial U}{\partial \eta}\right) + \frac{R_d}{a^2}J\left[\frac{T_v, \ln(p)}{\lambda, \mu}\right] = K\nabla^4\zeta + \mathbf{k}\cdot\nabla\times\mathbf{F}, \tag{4}$$

where the horizontal advection of absolute vorticity and "stretching term" $(2\Omega\mu + \zeta)D$ are combined into the divergence of the horizontal absolute vorticity flux $\nabla \cdot [\mathbf{V}(2\Omega\mu + \zeta)]$.

The baroclinic vorticity generation term will be neglected on the assumption that it is small everywhere except possibly over steep mountain slopes in the troposphere. At the chosen model level (close to 250 hPa), the term is certainly not expected to be any more significant that the term involving $\mathbf{F}$, which comes from subgrid-scale momentum transport parameterization. Over mountains peaking at a pressure of around 500 hPa, the model-level pressure is about 27 hPa lower than over sea points.

b. Coarse graining by spectral truncation

All flow variables in the IFS are available as spherical harmonic expansions and efficient spectral-to-gridpoint transforms exist that facilitate the calculation of nonlinear products by the grid-transform method.

Let the spectral expansion for ζ be given by

$$\zeta = \sum_{m=-\infty}^{\infty}\sum_{n=|m|}^{\infty}\zeta_n^m P_n^m(\mu)\exp(im\lambda) \tag{5}$$

and define the triangularly truncated expansion up to wavenumber N to be given by

$$[\zeta]_N = \sum_{m=-N}^{N}\sum_{n=|m|}^{N}\zeta_n^m P_n^m(\mu)\exp(im\lambda), \tag{6}$$

where $P_n^m(\mu)$ is the associated Legendre function, m is the zonal wavenumber, n is the degree [for which $n(n+1)/a^2$ is the total wavenumber squared], and ζ_n^m are the spherical harmonic coefficients, which satisfy the reality condition

$$\zeta_n^m = (-1)^m\overline{\zeta_n^{-m}}, \tag{7}$$

with the overbar denoting the complex conjugate.

Coarse graining a model field will be taken to mean spectral truncation to a lower wavenumber M so that

$$[[\zeta]_N]_M = [\zeta]_M, \tag{8}$$

with $M < N$. Using forecast fields from a high-resolution run truncated at $n = N$, the horizontal vorticity flux divergence term can be evaluated and then coarse grained to a lower resolution with truncation wavenumber M given by

$$[\nabla\cdot([\mathbf{V}]_N[\zeta]_N)]_M. \tag{9}$$

In a model forecast truncated at $n = M$, the horizontal vorticity flux divergence is $[\nabla\cdot([\mathbf{V}]_M[\zeta]_M)]_M$ and the difference between it and Eq. (9) can be regarded as a vorticity tendency error owing to the absence of spherical harmonic modes within the range $M < n < N$. If the operator $[\cdot]^{m,n}$ denotes projection onto the spherical harmonic with zonal wavenumber m and degree n (so that $[\zeta]^{m,n} = \zeta_n^m$) then

$$[\nabla\cdot([\mathbf{V}]_M[\zeta]_M)]^{m,n} - [\nabla\cdot([\mathbf{V}]_N[\zeta]_N)]^{m,n} \tag{10}$$

is the vorticity flux divergence "error" for the mode (m, n). From a wave–wave interaction viewpoint, this error term is the result of either two waves with $N \geq n > M$ interacting or the interaction of a mode having $n \leq M$, with a mode for which $N \geq n > M$.

It is instructive to separate the horizontal vorticity flux divergence into contributions from the rotational and divergent winds ($\mathbf{V}_\psi$ and $\mathbf{V}_\chi$, respectively). The former contribution can be identified with the advective term in

the barotropic vorticity equation, whereas the horizontal vorticity flux divergence by the divergent wind has been called the Rossby wave source (Sardeshmukh and Hoskins 1988).

Let the horizontal vorticity flux divergence by the rotational wind be $\mathrm{VFD}_N^{m,n}$, where

$$\mathrm{VFD}_N^{m,n} = [\nabla \cdot \{[\mathbf{V}_\psi]_N(2\Omega\mu + [\zeta]_N)\}]^{m,n} \qquad (11)$$

and the corresponding Rossby wave source $\mathrm{RWS}_N^{m,n}$ is given by

$$\mathrm{RWS}_N^{m,n} = [\nabla \cdot \{[\mathbf{V}_\chi]_N(2\Omega\mu + [\zeta]_N)\}]^{m,n}. \qquad (12)$$

Also, let $\mathrm{TIP}^{m,n}$ be the (m, n) spectral component of the sum of the terms involving $\dot{\eta}$ in Eq. (4). These terms describe vertical advection of vorticity and tipping of the horizontal vorticity into the vertical—hence the use of the abbreviation TIP.

Consider the following spectral representation of the vorticity equation in the IFS when truncated at $n = N$:

$$\frac{d\zeta_N^{m,n}}{dt} + \mathrm{VFD}_N^{m,n} + \mathrm{RWS}_N^{m,n} + \mathrm{TIP}_N^{m,n} = \mathrm{PAR}_N^{m,n} - K_N\left\{\frac{n(n+1)}{a^2}\right\}^2 \zeta_N^{m,n}, \qquad (13)$$

where $\mathrm{PAR}_N^{m,n}$ is the parameterization term. Now consider an equivalent representation for the vorticity equation in a spectral representation truncated to the lower wavenumber M:

$$\frac{d\zeta_M^{m,n}}{dt} + \mathrm{VFD}_M^{m,n} + \mathrm{RWS}_M^{m,n} + \mathrm{TIP}_M^{m,n} = -K_M\left\{\frac{n(n+1)}{a^2}\right\}^2 \zeta_M^{m,n} + R^{m,n}, \qquad (14)$$

with the requirement that

$$\zeta_M^{m,n} = \zeta_N^{m,n} \quad \text{for} \quad 0 \le n \le M, \qquad (15)$$

and where $R^{m,n}$ is a residual term that contains all of the forcing contributions from modes whose n satisfies the inequality $M \le n \le N$, together with an unspecified parameterization term.

In order for the low-resolution vorticity tendency to be corrected by the addition of the term $R^{m,n}$; that is, when

$$\frac{d\zeta_N^{m,n}}{dt} = \frac{d\zeta_M^{m,n}}{dt}, \qquad (16)$$

it follows that

$$R^{m,n} = \mathrm{PAR}_N^{m,n} + \mathrm{VFD}_M^{m,n} - \mathrm{VFD}_N^{m,n} + \mathrm{RWS}_M^{m,n} - \mathrm{RWS}_N^{m,n} + \mathrm{TIP}_M^{m,n} - \mathrm{TIP}_N^{m,n} + (K_M - K_N)\left\{\frac{n(n+1)}{a^2}\right\}^2 \zeta_M^{m,n}. \qquad (17)$$

Note that the terms involving the Coriolis parameter $2\Omega\mu$ are identical in the range $0 \le n \le M$ and so it is the relative vorticity flux divergence that requires evaluation.

Kinetic energy backscatter formulations tend to be formulated in terms of vorticity forcing functions (with the exception of the Met Office scheme, which also includes a horizontal divergence forcing term) and therefore are only concerned with rotational energy contributions to the total kinetic energy. Given the central role played by potential vorticity in numerical weather prediction and the dominance of the rotational energy over the contribution from the horizontal divergent wind, vorticity forcing would seem to be a natural basis for backscatter. Indeed, early unpublished work at ECMWF showed that backscatter of kinetic energy in the divergent wind was a highly ineffective means of perturbing forecasts, presumably because it excited gravity waves that were radiated into the stratosphere and dissipated. For this reason, the following analysis is focused entirely on rotational energy backscatter and the question of divergent energy forcing is left for future study. It is conceivable, however, that a similar analysis to the one carried out here could be quite revealing in respect to the upscale energy transfer into large-scale divergent wave modes in the tropics.

The rotational kinetic energy tendency $\partial\epsilon^{m,n}/\partial t$ in mode (m, n) is given by

$$\frac{\partial\epsilon^{m,n}}{\partial t} = -\overline{\psi^{m,n}}\frac{d\zeta_N^{m,n}}{dt} \qquad (18)$$

and so the rate of energy transfer from the wavenumber range $M \le n \le N$ into this wave mode is given by $-\overline{\psi^{m,n}}R^{m,n}$. For convenience, the following kinetic energy source terms will be defined; that is,

$$S_{\mathrm{VFD}}^{m,n} = -\overline{\psi^{m,n}}(\mathrm{VFD}_M^{m,n} - \mathrm{VFD}_N^{m,n}), \qquad (19)$$

$$S_{\mathrm{RWS}}^{m,n} = -\overline{\psi^{m,n}}(\mathrm{RWS}_M^{m,n} - \mathrm{RWS}_N^{m,n}), \qquad (20)$$

$$S_{\mathrm{TIP}}^{m,n} = -\overline{\psi^{m,n}}(\mathrm{TIP}_M^{m,n} - \mathrm{TIP}_N^{m,n}). \qquad (21)$$

3. Technical description of the calculation

It is important to understand that coarse graining is defined here to be spectral truncation of model fields to T159 resolution and that forecasts are only made at T1279 resolution for this purpose. However, T159 forecasts are used to compute the spectral distribution of biharmonic energy dissipation and stochastic kinetic energy backscatter (SKEB) energy input for comparison. Data for the calculation of the dynamical terms in the model's vorticity equation are obtained from 24-h forecasts at T1279 horizontal resolution (i.e., $N = 1279$) and 91 vertical levels. Vorticity and horizontal divergence are available in spectral form in the IFS and from those fields, the spectral-to-gridpoint transform was used to generate gridpoint fields of $\mathbf{V}_\psi$ and $\mathbf{V}_\chi$, as well as gridpoint fields of vorticity and horizontal divergence. From these fields, the vorticity fluxes by the rotational and divergent winds are computed and—in a single subroutine call—the spectral representation of the corresponding vorticity flux divergences are computed. Alongside this calculation, an identical calculation is performed on spectrally truncated representations of ζ and D—that is, spherical harmonic expansions up to $n = M$. To have about an order of magnitude reduction in resolution in the coarse-grained fields, M is chosen to be 159 (corresponding to a standard, lower-resolution configuration of the IFS). While this target resolution is considerably lower than current medium-range EPS resolutions (e.g., T639 at ECMWF), it is comparable with the resolutions often chosen for seasonal prediction and climate modeling.

The TIP requires $\dot{\eta}$, which is not available as a spectral field. It was derived here from the model's vertical velocity variable in gridpoint space (using the model's vertical coordinate definition) and then transformed to spectral space. Apart from that, the procedure to calculate TIP follows that for VFD and RWS. The horizontal diffusion term was evaluated directly from its corresponding spectral increment averaged over matching forecasts at T159 resolution.

The biharmonic diffusion coefficient used in the IFS horizontal diffusion scheme is 9 times smaller at T1279 resolution than at T159 and so K_N is essentially negligible in the above expression for $R^{m,n}$. The energy loss due to the diffusion term was calculated directly from the spectral vorticity increments.

Since this work is motivated by the need to provide justification for the use of SKEB schemes in ensemble prediction systems, it is interesting to compute the kinetic energy input by the ECMWF SKEB scheme (Palmer et al. 2009) in matching forecasts made at T159 resolution. Since this scheme applies vorticity increments in spectral space, it is very easy to calculate the distribution of energy input with respect to wavenumber n.

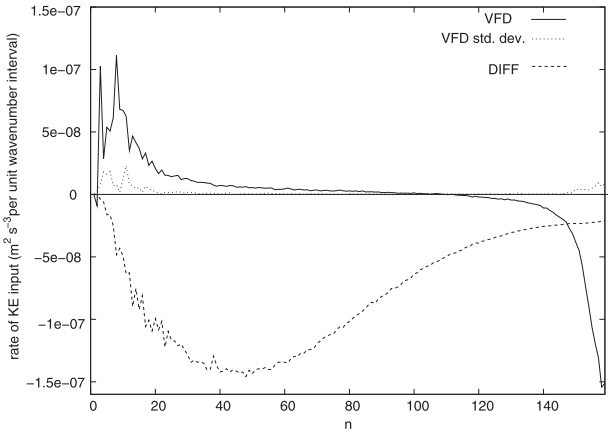

FIG. 1. Plot of S_{VFD} (solid), standard deviation of the daily mean about the 30-day mean (dotted line), and the dissipation rate due to horizontal diffusion (DIFF; dashed line) vs n at approximately 250 hPa.

The kinetic energy source terms are averaged over the 24-h forecast and summed over m for each value of n, so as to give the functions $S_{\mathrm{VFD}}(n)$, $S_{\mathrm{RWS}}(n)$, and $S_{\mathrm{TIP}}(n)$; for example,

$$S_{\mathrm{VFD}}(n) = \sum_{m=-n}^{m=n} S^{m,n}_{\mathrm{VFD}}. \tag{22}$$

The results are presented as averages over 30 forecasts made from 1200 UTC on each day between 1 and 30 January 2011. The IFS cycle used is 37R2.

4. Results

The kinetic energy source term due to the difference in vorticity advection by the rotational wind between the full and truncated representations $S_{\mathrm{VFD}}(n)$ is equivalent to the backscatter/drain term evaluated in the study by Thuburn et al. (2011). Figure 1 shows the average of $S_{\mathrm{VFD}}(n)$ at approximately 250 hPa from thirty 24-h forecasts together with the standard deviation of the daily values about the mean. Also, included is the corresponding spectral distribution of the energy sink due to biharmonic diffusion in the T159 forecasts. The form of $S_{\mathrm{VFD}}(n)$ is qualitatively very similar to that found by Thuburn et al. (2011) with strong energy sink for wavenumbers greater than 140 and a backscatter energy source that is largest between wavenumbers 5 and 30. Wavenumbers beyond the truncation wavenumber act as an energy sink for the wavenumber range 100–159 but particularly close to the truncation wavenumber. Backscatter is principally directed at the energy-containing

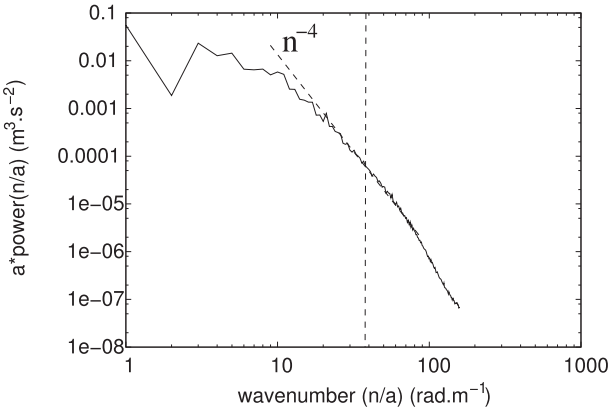

FIG. 2. Rotational kinetic energy spectrum in a T159 forecast showing the steep roll off beyond $n = 40$ where the slope approximates n^{-4}.

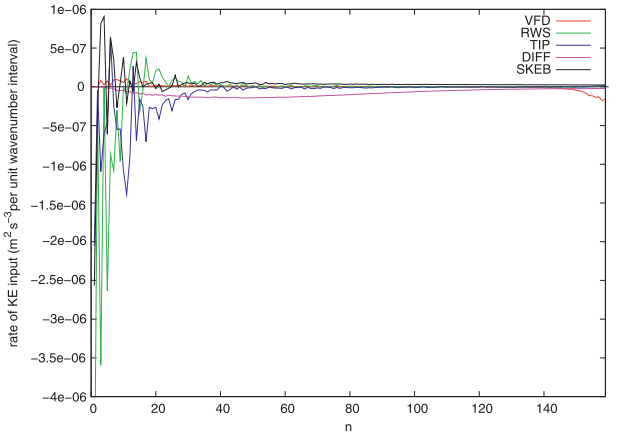

FIG. 3. Rate of kinetic energy input vs wavenumber for the individual components: $S_{\mathrm{VFD}}(n)$, $S_{\mathrm{RWS}}(n)$, and $S_{\mathrm{TIP}}(n)$ together with the energy sink due to horizontal diffusion and the energy source due to the SKEB scheme.

low wavenumbers and fits the vorticity straining model of 2D turbulence in which vorticity features are strained into small-scale filaments, exporting their energy to the straining flow while conserving enstrophy.

Somewhat surprising at first sight is the lack of scale selectivity of the biharmonic diffusion energy sink, which is largest near wavenumber 40. Since the energy sink due to biharmonic diffusion is proportional to $(\nabla\zeta)^2$, its spectral distribution is given by $n^2\Lambda(n)$, where $\Lambda(n)$ is the spectral enstrophy density. But $\Lambda(n) = n^2E(n)$, where $E(n)$ is the energy density and so the biharmonic energy sink is proportional to $n^2E(n)$. For the energy sink to decrease with increasing n, the spectral slope of the energy density must be steeper than n^{-4}.

Figure 2 shows some consistency with this statement and highlights the unrealistically steep slope of the energy spectrum (at 250 hPa), which at higher resolution (e.g., higher than T399) shows an n^{-3} midrange energy density dependence on wavenumber, which is in agreement with observations (Nastrom and Gage 1985). Of course, explicit diffusion is not the only dissipative process in the model and interpolation to the departure point in the semi-Lagrangian advection scheme acts as a smoother. In fact, McCalpin (1988) showed that cubic interpolation (as used in the IFS) is asymptotically similar to biharmonic diffusion. Clearly, what is required is a highly scale-selective hyperdiffusion scheme that replicates the energy drain seen close to the truncation wavenumber in Fig. 2. These findings entirely concur with those of MacVean (1983) who examined the effect of different hyperviscosity formulations on idealized baroclinic instability simulations and stability analyses. He concluded that biharmonic diffusion is too dissipative for numerical simulations with spectral truncations at least up to T95.

Figure 3 extends Fig. 1 to include the contributions from the Rossby wave source $S_{\mathrm{RWS}}(n)$, and the combined vertical advection and tipping term $S_{\mathrm{TIP}}(n)$, on a plot that greatly increases the range of the ordinate. Also included for reference, is the actual kinetic energy input obtained from the SKEB scheme for the 30 forecasts at T159. This is computed by multiplying the spectral components of the streamfunction forcing from SKEB by the corresponding spectral component of the model vorticity and then reversing the sign. As before, these are obtained as averages over every time step in the 24-h forecasts and then averaged over the 30 forecasts.

The first thing to note is that the term involving advection by the rotational wind $S_{\mathrm{VFD}}(n)$ is dwarfed by both the Rossby wave source term (which involves advection of vorticity by the divergent wind) and the tipping/vertical advection term $S_{\mathrm{TIP}}(n)$. Another striking feature is that $S_{\mathrm{TIP}}(n)$ is largely negative whereas $S_{\mathrm{RWS}}(n)$ is positive for wavenumbers greater than about 8. For $n > 40$, the SKEB KE input is remarkably uniform, apart from a gradual decrease toward large n but very noisy at low wavenumbers.

The above features are easier to see in Fig. 4, which spans the range $0 < n < 60$, together with reduced KE input range. For $n > 8$, the terms $S_{\mathrm{RWS}}(n)$ and $S_{\mathrm{TIP}}(n)$ tend to cancel so that the net effect of their sum over the entire wavenumber range is dissipative.

Given the apparent cancellation occurring between the terms $S_{\mathrm{RWS}}(n)$ and $S_{\mathrm{TIP}}(n)$, it is instructive to plot their sum (see Fig. 5). Clearly the overall effect of wavenumber contributions excluded by spectral truncation is a dissipative one.

The spectral energy tendency due to parameterized momentum forcing is shown in Fig. 6 together with the

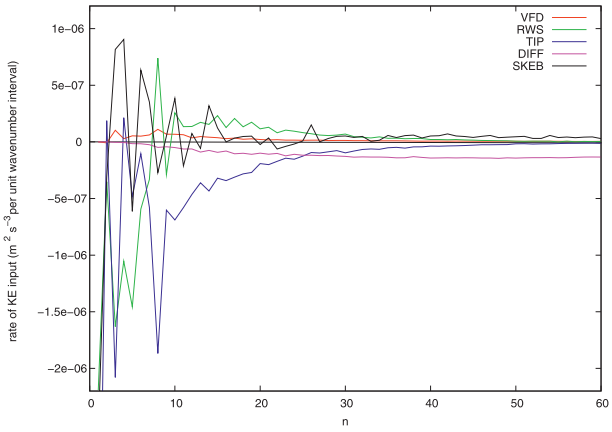

FIG. 4. As in Fig. 3, except zoomed in on the wavenumber range $0 \leq n \leq 60$ for clarity.

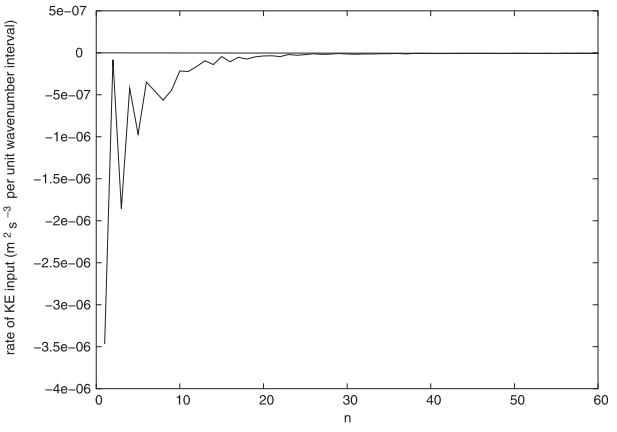

FIG. 5. Sum of $S_{\mathrm{RWS}}(n)$ and $S_{\mathrm{TIP}}(n)$ (denoted TIP).

sum of $S_{\mathrm{RWS}}(n)$ and $S_{\mathrm{TIP}}(n)$. This also is dissipative but now at least an order of magnitude larger than the sum of aforementioned explicit terms. When interpreting the significance of these terms to the parameterization problem for T159 resolution, one has to bear in mind their smallness relative to the parameterization term as it appears in the T1279 forecasts. Furthermore, in a practical NWP context, their effect would be lost in the tuning of the relevant parameterizations schemes (i.e., vertical diffusion, gravity wave drag, and cumulus momentum transport) for any particular resolution.

5. Discussion

The motivation for this research has been to identify kinetic energy backscatter as a large-scale dynamic process in the atmosphere and attempt to relate it to the use of stochastic backscatter in ensemble prediction systems. Ideally one would wish to calibrate the stochastic backscatter scheme directly but the calculations presented here do not distinguish between systematic and random backscatter forcing functions. These results draw attention away from the two-dimensional (or quasigeostrophic) turbulence view of upscale energy transport since coarse graining reveals that terms in the vorticity equation involving vertical velocity have much greater resolution sensitivity. While a clear backscatter signature is evident, as in the work of Thuburn et al. (2011), its contribution is small. More significant is the numerical diffusion term, which spuriously consumes energy in the subsynoptic scales and has no counterpart in the coarse-graining analysis. This, in itself, does not conflict with the raison d'etre for stochastic backscatter given by Shutts (2005), which was to counter spurious model dissipation.

The SKEB input seen in Fig. 3 certainly acts to oppose the biharmonic dissipation for wavenumbers greater than about 30. At lower wavenumbers, the global energy input due to SKEB requires a long period of time averaging before it settles down to its ensemble-mean value. This is because phase correlations between the streamfunction forcing and large-scale flow persist without months of averaging. The small standard deviation of $S_{\mathrm{VFD}}(n)$ shown in Fig. 1 suggests that the global-mean energy input in any 24-h period is nearly always positive, which is in marked contrast to the effect of SKEB. Figure 7 shows the modulus of $S_{\mathrm{RWS}}(n)$ together with its standard deviation. As for $S_{\mathrm{VFD}}(n)$, its standard deviation is much smaller than its mean for most wavenumbers. Therefore, it can be concluded that either SKEB has to be modified to increase phase correlation between the streamfunction forcing and the flow or a systematic backscatter forcing term should be added that inputs energy to large scales. This is perfectly

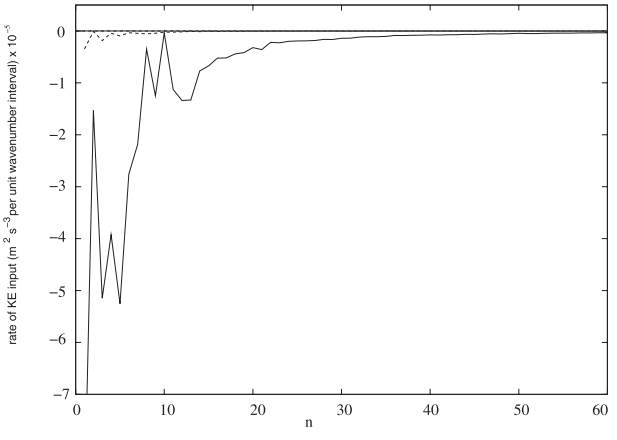

FIG. 6. Spectral distribution of KE dissipation due to model parameterization (solid) with the sum of S_{RWS} and S_{TIP} shown for reference (dashed). Note that units are $\mathrm{m}^2\ \mathrm{s}^{-3} \times 10^{-5}$.

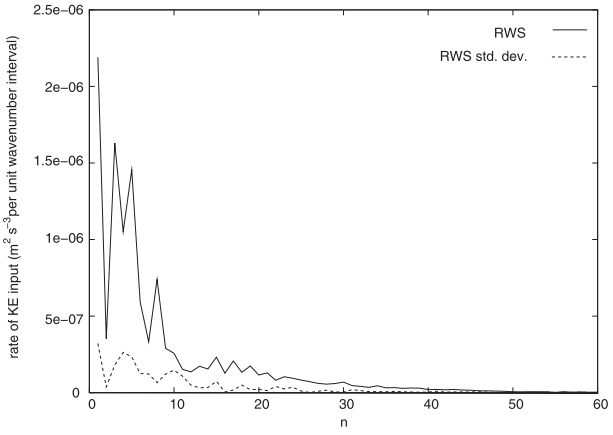

FIG. 7. $|S_{RWS}|$ (solid) and standard deviation of S_{RWS} (dashed) vs n.

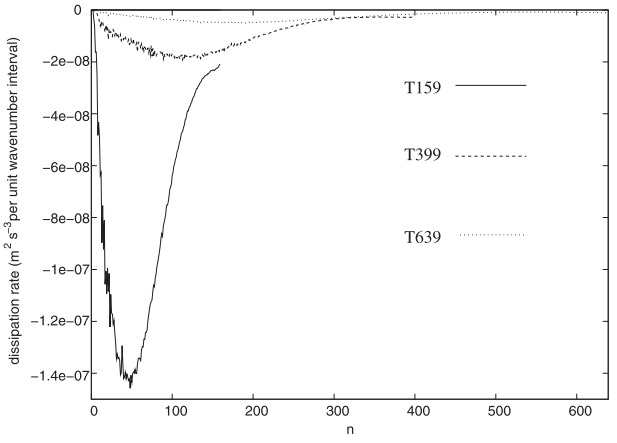

FIG. 8. Spectral distribution of KE dissipation rate (rotational flow only) at about 250 hPa for three model resolutions (T159, T399, and T639).

reasonable since it is well known that small-scale eddies become organized by large-scale flow structures and help maintain them. A possible candidate for this is the antidiffusive parameterization term ''vorticity confinement,'' which has been used recently to improve low-resolution climate simulation (Sanchez et al. 2013).

Figure 8 shows the spectral distribution of rotational kinetic energy dissipation by biharmonic diffusion for three different resolutions (T159, T399, and T639). The wavenumber of maximum energy dissipation rate moves from about 40 at T159 to about 110 at T399 and about 200 at T639. The maximum dissipation rate itself falls by a factor of 7 in going from T159 to T399 and then by another factor of 4 in going to T639. If the main function of SKEB was to balance this spurious numerical dissipation then one would expect the magnitude of SKEB forcing to decrease accordingly. However, the backscatter scheme also attempts to enhance the local upscale energy transport associated with deep convective systems—something unlikely to be revealed by the spectral diagnostics presented here.

While $S_{VFD}(n)$ is quite distinctive with its low wavenumber energy input and near-truncation-scale damping, contributions from other terms in the vorticity equation are dependent upon one another—as is seen in the cancellation between $S_{RWS}(n)$ and $S_{TIP}(n)$. Indeed, the term $S_{TIP}(n)$ is the sum of the vertical vorticity advection and the tipping term, which were already recognized to be closely linked. Their net effect at 250 hPa is to act as an energy sink at low wavenumbers, though for reasons that are not entirely clear. Since the IFS resolves inertia–gravity waves at T1279 (Shutts and Vosper 2011), it is possible that the energy sink is caused by wave drag due to waves emitted from the jet stream during geostrophic adjustment. Alternatively, it could be due to the effect of downgradient momentum transport by mesoscale motions in fronts or in regions of intense convection.

6. Conclusions

The effect of evaluating terms in the ECMWF IFS vorticity equation at two very different spectral truncations is used to determine the forcing effect of the omitted spectral wavenumber range. In this way, some quantification of kinetic energy backscatter could be achieved for an equivalent lower-resolution formulation of the model on the assumption that the full-resolution calculation was ''truth.'' The vorticity equation terms that form the basis of this study are grouped into the vorticity flux divergence by the rotational wind, the Rossby wave source, and the combined vertical advection of vorticity and tipping terms. Kinetic energy backscatter is clearly seen in the vorticity flux divergence associated with the rotational wind and is dominated by energy input into low wavenumbers, as found by Thuburn et al. (2011). This term is also responsible for an energy sink close to the truncation wavenumber (159) and very poorly parameterized by biharmonic horizontal diffusion. The ECMWF stochastic backscatter scheme run at T159 resolution qualitatively acts to offset the harmful effects of the horizontal diffusion although at low wavenumbers (<15, for instance), there is strong evidence to believe that a ''deterministic'' backscatter would be more appropriate than a stochastic one. This is because the daily-mean kinetic energy input at these wavenumbers from both the VFD and RWS terms is quite steady and positive whereas the SKEB term fluctuates wildly.

The Rossby wave source term is positive for all but the lowest wavenumbers but this energy input is

counteracted by an energy sink associated with the combined vertical advection and tipping terms and so their net effect is dissipative. Furthermore, the size of this net dissipative effect is much greater than the KE backscatter coming from the VFD term. Even so, in the global mean at least, these terms only represent a small correction to the parameterization term in Eq. (17). One could argue that by taking a global, spectral view, the importance of intense local backscatter events has been lost in global averaging. The spectral analysis is, however, appropriate to the study of the performance of operational stochastic backscatter schemes, which mostly have a spectral formulation.

It may be that the scope of these results is too small to draw firm recommendations for stochastic backscatter parameterization but, along with the results of Thuburn et al. (2011), it would appear that the need for backscatter should decrease rapidly with increasing resolution. Not only does the computed backscatter fall sharply with increasing resolution, the dissipation rate associated with biharmonic diffusion also falls rapidly and gets spread over a wider wavenumber range. The direct effect of numerical diffusion on the energy-containing scales (say, $n < 60$) falls off even faster because of this spreading. Given the dominance of the parameterization term in the vorticity equation and the likely importance of neglected statistical fluctuations in its formulation, parameterized momentum transport would seem to be a more plausible source of model error than stochastic backscatter.

The target resolution for this study (T159) is coarser than that used in current operational EPS but was chosen to be almost an order of magnitude smaller than the highest affordable resolution (T1279) to ensure stable coarse-graining statistics. Future studies will aim to use a target resolution comparable with operational EPS and attempt to decompose the terms into systematic and random components. In this way it should be possible to verify and calibrate the backscatter formulation, or replace it with a formulation that better reflects the real uncertainty in the model's momentum equation.

Acknowledgments. I am happy to acknowledge the technical assistance provided by Martin Leutbecher and Martin Steinheimer at ECMWF during the course of this work. The project was supported equally by the Met Office and ECMWF as part of a collaboration on stochastic physics.

REFERENCES

Berner, J., G. J. Shutts, M. Leutbecher, and T. N. Palmer, 2009: A spectral stochastic kinetic energy backscatter scheme and its impact on flow-dependent predictability in the ECMWF Ensemble Prediction System. *J. Atmos. Sci.,* **66,** 603–626.

Charron, M., G. Pellerin, L. Spacek, P. L. Houtekamer, N. Gagnon, H. L. Mitchell, and L. Michelin, 2010: Toward random sampling of model error in the Canadian Ensemble Prediction System. *Mon. Wea. Rev.,* **138,** 1877–1901.

Frederiksen, J. S., and A. G. Davies, 1997: Eddy viscosity and stochastic backscatter parameterizations on the sphere for atmospheric circulation models. *J. Atmos. Sci.,* **54,** 2475–2492.

Kitsios, M., J. S. Frederiksen, and M. J. Zidikheri, 2012: Subgrid model with scaling laws for atmospheric simulations. *J. Atmos. Sci.,* **69,** 1427–1445.

Leith, C., 1990: Stochastic backscatter in a subgridscale model: Plane shear mixing layer. *Phys. Fluids,* **2A,** 297–299.

MacVean, M. K., 1983: The effects of horizontal diffusion on baroclinic development in a spectral model. *Quart. J. Roy. Meteor. Soc.,* **109,** 771–783.

Mason, P. J., and D. J. Thomson, 1992: Stochastic backscatter in large-eddy simulations of boundary layers. *J. Fluid Mech.,* **242,** 51–78.

McCalpin, J. D., 1988: A quantitative analysis of the dissipation inherent in semi-Lagrangian advection. *Mon. Wea. Rev.,* **116,** 2330–2336.

Nastrom, G. D., and K. S. Gage, 1985: A climatology of atmospheric wavenumber spectra of wind and temperature observed by commercial aircraft. *J. Atmos. Sci.,* **42,** 950–960.

Palmer, T. N., R. Buizza, F. Doblas-Reyes, T. Jung, M. Leutbecher, G. J. Shutts, M. Steinheimer, and A. Weisheimer, 2009: Stochastic parametrization and model uncertainty. ECMWF Tech. Memo. 598, 42 pp.

Sanchez, C., K. D. Williams, G. J. Shutts, R. E. McDonald, T. J. Hinton, C. A. Senior, and N. Wood, 2013: Towards the development of a robust model hierarchy: Investigation of dynamical limitations at low resolution and possible solutions. *Quart. J. Roy. Meteor. Soc.,* **139,** 75–84.

Sardeshmukh, P. D., and B. J. Hoskins, 1988: The generation of global rotational flow by steady idealized tropical divergence. *J. Atmos. Sci.,* **45,** 1228–1251.

Shutts, G. J., 2005: A kinetic energy backscatter algorithm for use in ensemble prediction systems. *Quart. J. Roy. Meteor. Soc.,* **131,** 3079–3102.

——, and S. B. Vosper, 2011: Stratospheric gravity waves revealed in NWP model forecasts. *Quart. J. Roy. Meteor. Soc.,* **137,** 303–317, doi:10.1002/qj.763.

Tennant, W. J., G. J. Shutts, A. Arribas, and S. A. Thompson, 2011: Using a stochastic kinetic energy backscatter scheme to improve MOGREPS probabilistic forecast skill. *Mon. Wea. Rev.,* **139,** 1190–1206.

Thuburn, J., J. Kent, and N. Wood, 2011: Energy and enstrophy cascades in numerical models. *Proc. Workshop on Representing Model Uncertainty and Error in Numerical Weather and Climate Prediction Models,* Reading, United Kingdom, ECMWF, 53–64.